Title
Examination of laser-induced cell lysis by time resolved imaging

Authors
Rau, KR
Guerra, A
Vogel, A
et al.

Publication Date
2004-10-27

DOI
10.1117/12.529622

Examination of laser-induced cell lysis by time resolved imaging

Kaustubh R. Rau[a,b], Arnold Guerra III[b,c], Alfred Vogel[d] and Vasan Venugopalan[a,b,c,*]
[a]Dept. of Biomedical Engineering, University of California, Irvine, CA 92697
[b]Dept. of Chemical Engineering and Materials Science, University of California, Irvine, CA 92697
[c]Laser Microbeam and Medical Program, Beckman Laser Institute, University of California, Irvine, CA 92697
[d]Medical Laser Centre Lübeck, Peter Monnig Weg 4, D-23562, Lübeck, Germany.

ABSTRACT

Highly focused laser microbeams are being used with increasing regularity for targeted cell lysis, cellular microsurgery and molecular delivery via transient cell membrane permeabilization. To examine the mechanisms of laser induced cell lysis, we performed time-resolved imaging of confluent PtK2 cell cultures following the delivery of a single 6 ns, 532 nm Nd:YAG laser pulse. The laser pulse energies employed correspond to 1x and 3x threshold for plasma formation. The resulting plasma formation, pressure wave propagation and cavitation bubble dynamics were imaged over a temporal range spanning 5 orders of magnitude (0.5 ns – 50 μs). Time-resolved imaging enabled determination of process characteristics including pressure wave speed and amplitude and cavitation bubble energies. The time-resolved images also revealed the onset of cellular damage to occur on nano-second time scales and complete within 1 μs. Moreover, the size of the damage zone was larger than the plasma but smaller than the maximum cavitation bubble size. This indicated that mechanisms apart from plasma vaporization namely pressure wave propagation and cavitation bubble expansion are contributors to cellular damage. Dye exclusion assays showed that the majority of cells experiencing considerable deformation due to fluid flow generated by the cavitation bubble expansion remain viable over 24 hours.

Keywords: cell lysis, laser scissors, microsurgery, plasma, pressure wave, cavitation bubble

1. INTRODUCTION

Optical tools such as laser scissors and tweezers are now viewed as integral techniques in the biologists tool-kit for perturbing biological systems on the molecular and cellular level[1]. The use of laser tweezers in measuring mechanical properties of cells and biomolecules with sensitivity in the pico- to femtonewton range is well established[2]. There has also been a proliferation in the use of pulsed laser microbeams for selective cell lysis[3], intracellular microsurgery[4], gene inactivation[5] and cell transfection via transient permeabilization of the plasma membrane[6,7]. Several factors have contributed to the interest in using pulsed laser microbeams for biological applications including development of alternatives to harsher transfection methods like detergents, micro-pipettes and electroporation, selective targeting abilities capable of generating nanometer scale effects and ease of integration on microfluidic chip platforms for biochemical analysis and single cell analytics. An understanding of the laser-cell interaction is crucial to the progression of pulsed laser microbeams from research tools to useable analytical techniques. Outstanding issues include

* vvenugop@uci.edu; Phone: 949 - 824 - 5802; Fax: 949 - 824 - 2541

Imaging, Manipulation, and Analysis of Biomolecules, Cells, and Tissues II,
edited by D. V. Nicolau, J. Enderlein, R. C. Leif, D. L. Farkas, Proc. of SPIE Vol. 5322
(SPIE, Bellingham, WA, 2004) · 1605-7422/04/$15 · doi: 10.1117/12.529622

the understanding of photo-damage mechanisms and the determination of optimal irradiation parameters (wavelength, pulse durations and energy) for a given application.

Although the use of pulsed laser microbeams with pulse durations ranging from nano- to femtoseconds have been described the mechanisms of cell lysis or transfection are not as well studied. Venugopalan and co-workers recently established that pulse energies and irradiances used to produce laser-induced breakdown in water using 6 ns pulses at λ = 532 and 1064 nm focused at high numerical aperture are similar to those used in techniques like cell lysis and optoporation[8]. Thus it was hypothesized that laser-induced breakdown is the mechanism responsible for laser cell lysis, microsurgery and optoporation/injection. While laser-induced breakdown in a pure medium such as water[9,10] as well as laser-induced cell lysis of cells loaded with light absorbing micro- and nano-particles have been imaged[11], there have been no studies that visualize cell lysis produced by laser-induced plasma formation in *in-vitro* cell cultures. We thus developed a time-resolved imaging system to image the cell lysis process upon delivery of a single nanosecond laser pulse focused at high numerical aperture into a plated cell sample.

2. MATERIALS AND METHODS

2.1 Experimental Setup

A schematic of the imaging setup used in the experiments is shown in Fig. 1. A 6 ns duration, λ = 532 nm Nd: YAG laser (Brilliant B, Quantel Inc., Big Sky Laser MT) was introduced via the back aperture of a 40x objective (Zeiss Achroplan, *NA* = 0.8) to produce cell lysis. Time-delayed pulses for illumination purposes were produced by two different means. For time delays spanning 0.5 ns to 1 μs, the laser output was split with one beam being sent to the microscope to produce cell lysis and the other being used to excite fluorescence in a dye solution (LDS 722, Exciton Inc.). The dye fluorescence was collected by a multimode fiber optic line (600 UMT, Thor Labs) with the output being coupled into the microscope condenser. The length of the fiber optic line determined the delay between the irradiation and illumination pulses arriving at the cell sample. The bandwidth of the fluorescence emission ($\Delta\lambda$ ~ 40 nm) eliminated speckle in the image. For imaging on time scales longer than 1 μs, we utilized an ultrashort pulse duration (Δt ~ 20 ns) flash lamp (Nanolite KL-L, High Speed Photo Systeme, Germany) that was triggered by a TTL pulse from the Nd: YAG laser Q-switch at an appropriate time using a delay generator (DG535, Stanford Research Systems). An intensified gated CCD camera (PI-Max, Roper Scientific Inc.) used for image collection was also triggered by a TTL pulse from the Nd: YAG laser Q-switch. A long pass filter (LP 570, Omega Optics) was used to block stray laser radiation from reaching the camera. Camera gate widths of 0.5 ns were used for dye fluorescence illumination and 200 ns for flash lamp illumination. This imaging system enabled the imaging of the dynamics of laser-induced breakdown in cell cultures including plasma generation, pressure wave propagation and cavitation bubble expansion and collapse.

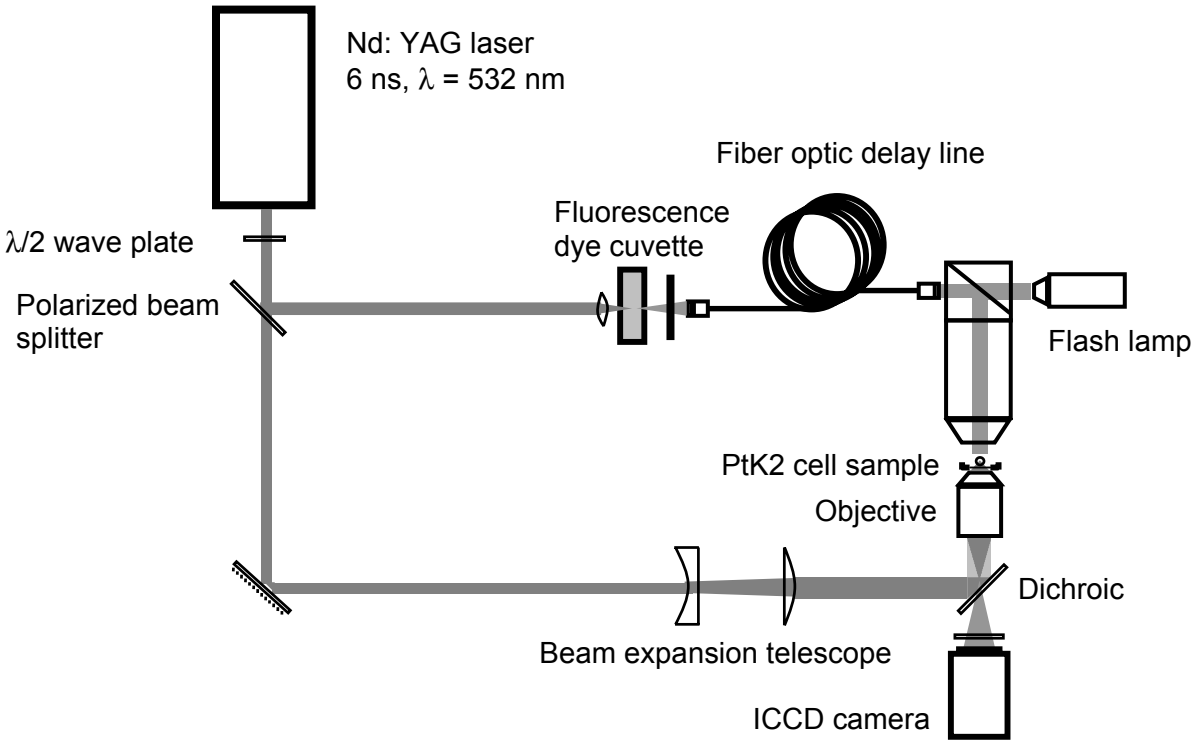

Fig. 1. Schematic of the experimental setup for time resolved imaging.

2.2 Cell Culture and Fluorescence Microscopy

Potorous rat kidney epithelial cells (PtK2) plated on imaging dishes were used as the sample. Cell lines were grown and maintained using standard cell culture techniques in phenol-red free culture medium. Cell viability after laser irradiation was assessed using a combined Acridine Orange (AO) and Propidium Iodide (PI) assay. AO is a nuclear stain readily taken up by cells and used to assess cell viability while PI is a membrane impermeant dye which is taken up by cells if the plasma membrane is compromised with uptake being an indication of dead or apoptotic cells.

2.3 Measurement of Plasma Threshold

Prior to cell irradiation the threshold for plasma generation was determined for phenol-red free culture medium in an imaging dish. Laser pulses were focused into culture medium and plasma generation was observed visually in a darkened room. Plasma incidence at a particular pulse energy was observed for 50 pulses and the threshold was defined as the pulse energy needed to achieve a 50% probability of plasma generation. Fig. 2 shows the plot for plasma incidence as a function of pulse energy with threshold being approx. 8 μJ. Cell samples were irradiated at pulse energies corresponding to 1x and 3x threshold and time-resolved images were taken of the lysis process. The laser focus was positioned slightly above (< 5 μm) the plated cells and into the culture medium.

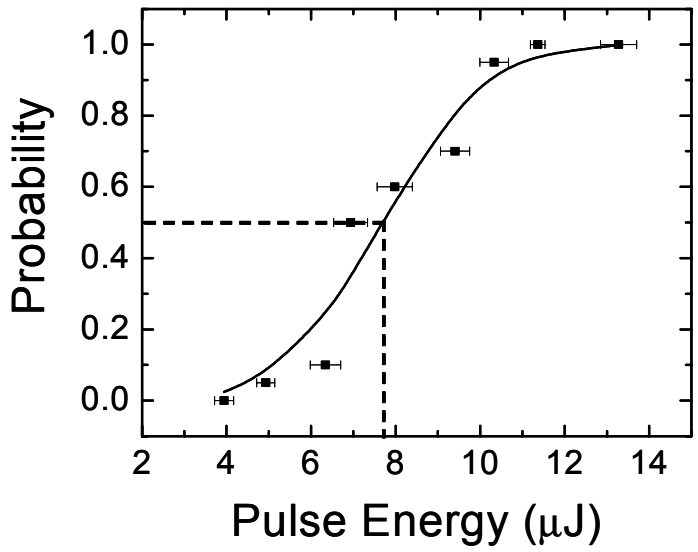

Fig. 2. Probability of plasma incidence as a function of pulse energy. The threshold for 50% plasma formation is approx. 8 μJ and marked with the dotted line.

3. RESULTS AND DISCUSSION

Fig. 3 shows images of PtK2 cell cultures at various time points after irradiation by a laser pulse with pulse energy at 3x threshold. Each image corresponds to a different time point after a single pulse was focused into the cell sample. The images clearly show the progression of cell lysis produced by laser induced breakdown. Fig. 3(a) is an image taken at a time delay of 20 ns and shows the maximum plasma size and the pressure wave launched by the rapid plasma expansion. After 20 ns, the plasma luminescence is no longer seen and a cavitation bubble resulting from the plasma expansion is found (fig. 3b). The pressure wave has also propagated a larger distance. It is remarkable that the passage of this pressure wave through the cell sample did not cause any visually observable cellular damage since it is known maximum pressures in the range of 100 MPa – 1 GPa are generated in optical breakdown[8]. The onset of cellular damage is clearly seen inside the cavitation bubble indicating that lysis starts on the nanosecond time scale. Fig. 3(c) shows the rapid bubble expansion at a later points and the associated propagation of the region of cell lysis. The lysis process results in a clear zone around the irradiation site with cellular debris visible inside the bubble. Cell lysis appears to be caused by shear stresses generated by outward fluid movement associated with the bubble expansion. However, cell lysis is only observed upto approx. 1 μs, even though the bubble expansion continues upto 20 – 45 μs. This can be clearly seen in fig. 3(d) where the bubble expansion only encompasses the surrounding cells without lysing them. The region of cell lysis can be clearly seen in the center of the image. Another interesting feature is the considerable deformation experienced by the cells that remain intact as seen in fig. 3(d). The bubble collapse does not appear to produce any additional damage, but only serves to clear away the cellular debris.

The time-resolved imaging allowed measurement of the maximum bubble size R_{max} and bubble oscillation time T_{osc}. These parameters were used to calculate bubble energy. Assuming a hemispherical

bubble expansion (due to the cover slip boundary of the imaging dish), bubble energy E_B maybe expressed as[9, 10]

$$E_B = \frac{1}{2} \times \frac{4}{3} \pi \rho_0 \left(\frac{2 \times 0.915}{T_{osc}} \right)^2 R_{\max}^5$$

with ρ_0 being the density of the medium (1000 kg/m^3). The values for R_{max}, T_{osc} and E_B for irradiation 1x and 3x threshold are given in table 1.

Table 1. Laser pulse energy (E_P), maximum cavitation bubble radius (R_{max}), bubble oscillation time (T_{osc}), bubble energy (E_B) and conversion efficiency for 1x and 3x threshold.

	$E_P(\mu J)$	R_{max} (μm)	T_{osc} (μs)	E_B (μJ)	E_B / E_P
1x Threshold	8	118	20	0.4	5 %
3x Threshold	24	220	40	2.26	9.4 %

As the pulse energy increases the conversion into bubble energy also increases. This is seen by the increase in conversion efficiency from 10 to 19% for irradiation at 1x and 3x threshold respectively. The maximum bubble sizes and bubble oscillation times are also correspondingly larger. The larger bubble sizes also cause an increase in the zone of lysis.

The viability of the remaining cells were also evaluated by fluorescence microscopy. Fig. 4 shows the results of viability testing using AO and PI stains. Fig. 4(a) shows the cell sample in phase contrast with the the lysis zone as marked. Fig. 4(b & c) show fluorescence images of the same field of cells. Fig. 4(b) shows that nearly all the cells which were deformed due to the bubble expansion withstand this mechanical stress and are still viable (AO stain). These cells were also followed 24 hours post irradiation and continued to remain viable. Fig. 4(c) shows that only cells surrounding the lysis zone take up PI, indicating that their plasma membrane is compromised.

4. CONCLUSIONS

Irradiation with a single focused nanosecond laser pulse produced laser-induced breakdown within confluent PtK2 cell cultures. Time resolved imaging enabled visualization of the processes involved in laser-induced cell lysis. The experimental setup provided images over the interval of 0.5 ns to 50 μs. Cavitation bubble expansion was the major contributor to cell lysis. Cells also demonstrated the ability to withstand deformation produced by the fluid flow associated with bubble expansion and remain viable.

ACKNOWLEDGEMENTS

We acknowledge support from the National Institutes of Health via the Laser Microbeam and Medical Program (NIH-P41-RR-01192) and Bioengineering Research Partnership Program (NIH-R01-RR-14892).

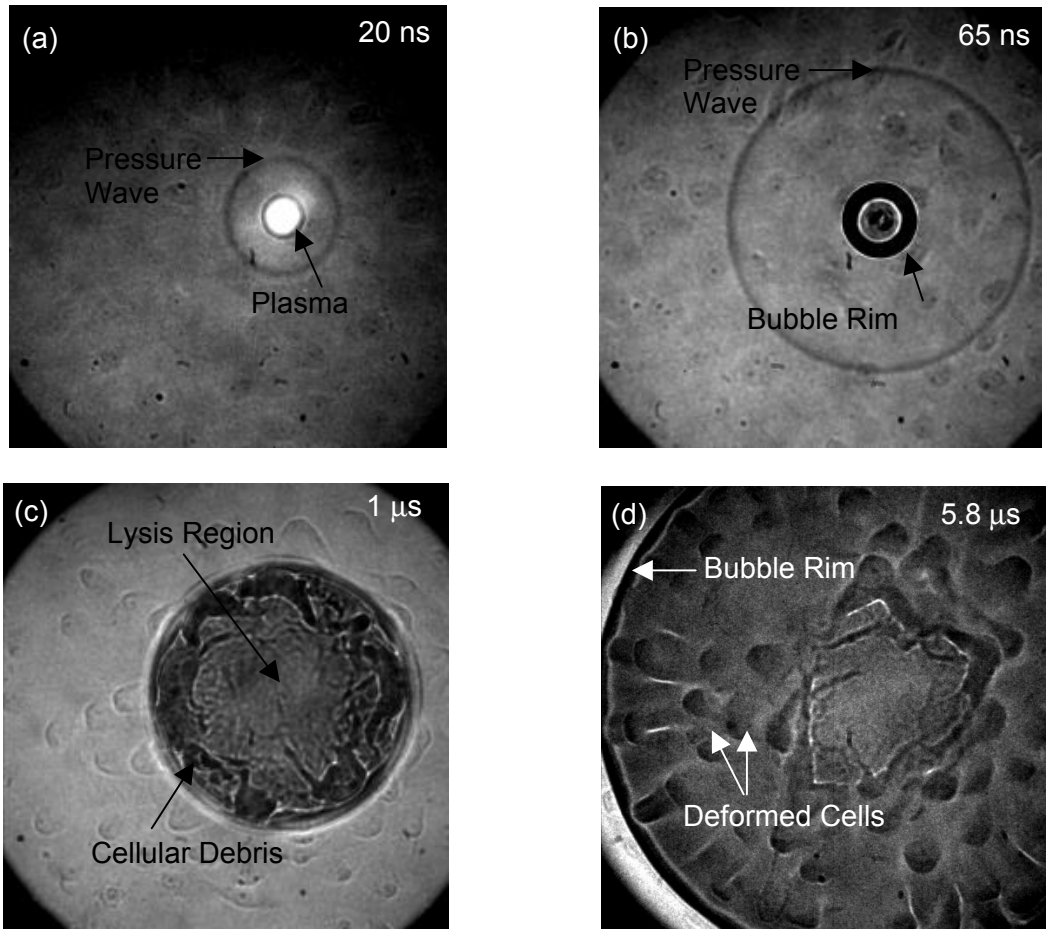

Fig. 3. Time resolved images series of laser induced cell lysis at 3x threshold pulse energy. The different features of the lysis process are marked on each image.

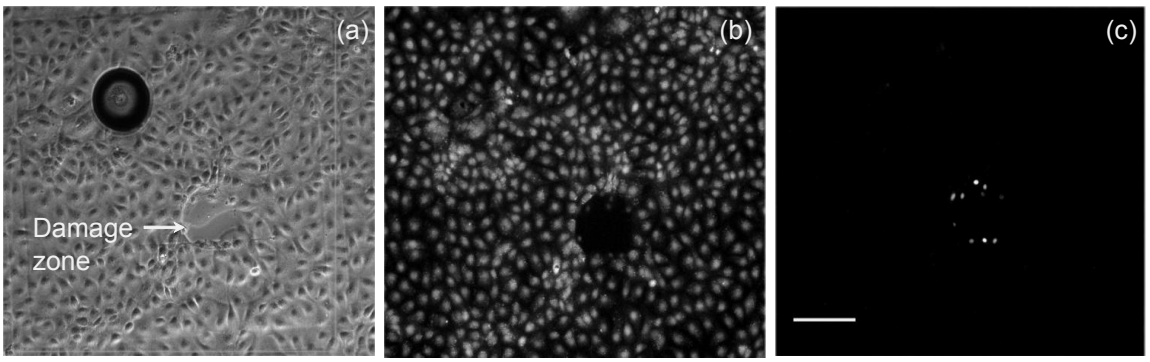

Fig. 4. Cell viability assay post irradiation: (a) phase contrast image showing the irradiation site and damage zone, (b) fluorescence image with acridine orange staining showing viable cells and (c) propidium iodide staining showing dead cells around the periphery of the irradiation site. Scale bar = 200 µm.

REFERENCES

1. K . Schütze, I Becker, K. F. Becker, S. Thalhammer, R. Stark, W. M. Heckl, M. Bohm and H. Posl. Cut out or poke in--the key to the world of single genes: laser micromanipulation as a valuable tool on the look-out for the origin of disease, *Genet Anal.* 14, 1 (1997).
2. S. C. Kuo. Using optical forces to measure biological forces and mechanics, *Traffic* 2, 757 (2001).
3. C. M. Pitsillides, E. K. Joe, X. Wei, R. R. Anderson and C. P. Lin. Selective cell targeting with light-absorbing microparticles and nanoparticles, *Biophys. J.* 84, 4023 (2003).
4. A. Khodjakov, R. W. Cole and C. L. Reider. A Synergy of Technologies: Combining Laser Microsurgery with Green Fluorescent Protein tagging, *Cell Motil. Cytoskel.* 38, 311 (1997).
5. M. Berns, Z. Wang, A. Dunn, V. Walllace and V. Venugopalan. Gene inactivation by multiphoton-targeted photochemistry, Proc. Natl. Acad. Sci. 97, 9504 (2000).
6. T. B. Krasieva, C. F. Chapman, V. J. LaMorte, V. Venugopalan, M. W. Berns and B. J. Tromberg. Cell permeabilization and molecular transport by laser microirradiation, *Proc. SPIE* 3260, 38 (1998).
7. J. E. Soughayer, T. B. Krasieva, S. C. Jacobson, J. M. Ramsey, B. J. Tromberg and N. L. Allbritton. Characterization of cellular optoporation with distance, *Anal. Chem.* 72, 1342 (2000).
8. V. Venugopalan, A. Guerra, K. Nahen and A. Vogel. Role of laser-induced plasma formation in pulsed cellular microsurgery and micromanipulation, *Phys. Rev. Lett.* 88, 078103 (2003).
9. A. Vogel, S. Busch and U. Parlitz. Shock wave emission and cavitation bubble generation by picosecond and nanosecond optical breakdown in water, *J. Acoust. Soc. Am.* 100, 148 (1996).
10. C. B. Schaffer, N. Nishimura, E. N. Glezer, A. M.-T. Kim and E. Mazur. *Opt. Exp.* 10, 196 (2002).
11. C. P. Lin, N. W. M. Kelly, S. A. B. Sibayan, M. A. Latina, and R. R. Anderson. Selective cell killing by microparticle absorption of pulsed laser radiation, *IEEE J. Selected Top. Quant. Electron.* 5, 963 (1999).